# Different life strategies of the three commercially exploited scallop species living under the same environmental conditions

Daria Ezgeta-Balić[1], Melita Peharda[1]*, Bernd R. Schöne[2], Hana Uvanović[1], Nedo Vrgoč[1], Krešimir Markulin[3], Ivana Radonić[1], Cléa Denamiel[4] and Žarko Kovač[5]

[1]Laboratory of Fisheries Science and Management, Institute of Oceanography and Fisheries, Split, Croatia, [2]Institute of Geosciences, University of Mainz, Mainz, Germany, [3]Laboratory of Chemical Oceanography and Sedimentology of the Sea, Institute of Oceanography and Fisheries, Split, Croatia, [4]Laboratory for Physical Chemistry of Aquatic Systems, Division for Marine and Environmental Research, Ruđer Bošković Institute, Zagreb, Croatia, [5]Department of Physics, Faculty of Science, University of Split, Split, Croatia

To understand the response of marine species to a changing environment, it is crucial to have deep insight into their main biological traits. This study used a multi-species approach to comparatively analyse the reproductive and growth strategies of three commercially important scallop species. Target taxa were larger sized Mediterranean scallop *Pecten jacobeaus*, and two smaller sized species *Aequipecten opercularis* and *Flexopecten glaber*. Specimens were collected at approximate monthly intervals from February 2017 to October 2018 from a commercial beam trawl in the northern Adriatic area (west coast of the Istria peninsula, 25-35 m depth). Three different complementary methods were applied to obtain comprehensive knowledge about the reproductive cycle including assessment of the gonadosomatic index (GSI), histological analysis of gonad tissue, and measuring oocyte size. Growth strategies of three target species were analyzed using high-resolution stable oxygen isotope data that were temporally aligned on sea water temperature data obtained by AdriSC ROMS model. Results indicate diverse strategies employed by these taxonomically related species exposed to the same environmental conditions. *Pecten jacobaeus* spawned in the late summer and early fall, while shell growth slowed down during warmer season. *Aequipecten opercularis* spawned in the winter and slowed down shell deposition process during the cold season. Spawning of *F. glaber* occurred during early to mid-summer and growth slowed down during warmer season. This study provides an important scientific baseline for sustainable management and future aquaculture attempts of scallops.

KEYWORDS

Mediterranean scallop, queen scallop, smooth scallop, histology, gonadosomatic index, oxygen stable isotope, growth rate, Adriatic

# Introduction

Scallops are a globally distributed group of epibenthic bivalves (Shumway and Parson, 2016). They have been a prominent research target for more than a century (e.g., Fullarton, 1896) because many species are commercially important (for a review see Shumway and Parson, 2016, and chapters within). Scallops react sensitively to environmental changes (e.g., Cooley et al., 2015; Stokesbury and Bethoney, 2020; Ramos et al., 2022) and global change including acidification, seawater temperature rise and/or hypoxia can have deleterious effects on scallop populations (Talmage and Gobler, 2011; Gobler et al., 2014; Clements and Hunt, 2017). Besides environmental conditions, commercially important species are under uninterrupted fishing pressure, which also cause changes in the bivalve population (Duncan et al., 2016).

Scallop fisheries are very abundant in the European Union (EU) with *Pecten maximus* and *Aequipecten opercularis* as the most important species. Other scallop taxa are mostly of regional importance including *Chlamys islandica* in the northern, sub-arctic areas of Europe, and *Pecten jacobaeus*, *Mimachlamys varia*, and *Flexopecten glaber* in the Mediterranean Sea (Duncan et al., 2016). The main fishing area for *P. jacobaeus* in the Mediterranean region is the northern Adriatic Sea, where both Italian and Croatian fishermen exploit this species with beam trawlers. According to Eurostat, after Italy, with approx. 40 tonnes in 2020, Croatia caught the second largest amount of *P. jacobaeus* among all EU countries. However, landings of *P. jacobaeus* in Croatia decreased significantly in the last five years (Eurostat). Consequently, the economic importance of other small scallop species started to increase, including *A. opercularis* and *F. glaber*, which were previously mainly considered as non-commercial discard (Ezgeta-Balić et al., 2021). Knowledge of the main biological traits of the exploited scallop species is crucial to understanding their possible response to a changing environment. Considering the economic importance of *P. jacobaeus*, changes in their main biological traits, such as growth and reproduction, are essential issues in ecological and economic contexts.

Unlike the great scallop, *P. maximus*, which was the focus of many previous studies (e.g., Laing, 2002; Chauvaud et al., 2005; Andersen et al., 2011; Chauvaud et al., 2012; Lavaud et al., 2014; Götze et al., 2020; Fröhlich et al., 2022; Thébault et al., 2022), scientific research on *P. jacobaeus* is relatively limited (e.g., Mattei and Pellizzato, 1996; Peharda et al., 2003; Katsanevakis, 2005; Marguš and Teskeredžić, 2005; Peharda et al., 2019). Based on genetic studies, some authors suggested that these two species could represent a single species or races/subspecies (Wilding et al., 1999; Saavedra and Peña, 2004; Saavedra and Peña, 2005; Morvezen et al., 2016; Vendrami et al., 2019) as their phylogenetic status is not completely clear. However, further genetic studies need to be performed to clarify the status of both taxa. According to the World Register of Marine Species (https://www.marinespecies.org; last access: 2 June 2022), the two taxa are still considered as different species.

According to Peharda et al. (2003), *P. jacobaeus* can attain a lifespan of 13 years, while minimum conservation reference sizes of 10 cm are reached between the third and fourth year of life. The largest reported specimen had a shell length of 15 cm long (Cetinić and Soldo, 1999). A stock assessment of *P. jacobaeus* was only performed for the western Adriatic Sea indicating that the state of the biomass was still below the $B/B_{MSY}$ reference point despite a slight decrease in fishing mortality in more recent times (Armelloni et al., 2021). Therefore, knowledge of the ecological baseline of *P. jacobaeus* is important for its protection and sustainable management. Although shell growth of *P. jacobaeus* was recently investigated by Peharda et al. (2019), the study did not account for important biological traits that could impact growth dynamics. Reproduction is one of the essential biological traits, but it is poorly investigated for this species. Most of the existing publications are outdated (e.g., Castagnolo, 1991) and do not consider changes in the marine environment during the last two decades.

Due to its wide distribution range and commercial value in some regions, the queen scallop *A. opercularis* is well-studied, but mostly just the Atlantic populations (e.g., Heilmayer et al., 2004; Johnson et al., 2021). This species occurs along the European Atlantic coast, Mediterranean, and Black Sea. *Aequipecten opercularis* is most common at depths of around 40 m, but can be found at depths ranging from the intertidal zone to 400 m (Poppe and Goto, 2000). Similar to *P. jacobaeus*, the state of the biomass of *A. opercularis* in the western Adriatic is still below the $B/B_{MSY}$ reference point (Armelloni et al., 2021), although it has been exploited for a long time in this region. The distribution of the other small scallop species, *F. glaber*, is mainly limited to the Mediterranean Sea, as it rarely occurs in the Atlantic Ocean (Poppe and Goto, 2000). Recent studies provide information on the biology of *F. glaber* (e.g., Marčeta et al., 2016; Nardi et al., 2018; Shcherban and Melnik, 2020), but in general, it is poorly studied. Compared with *P. jacobaeus*, these two species are short-lived and fast-growing bivalves, making them potentially good candidates for aquaculture (Román et al., 1999; Marčeta et al., 2016).

In this study, we conducted a comparative multi-species analysis of the three commercially important scallop species living under the same environmental conditions, namely, the Mediterranean scallop *Pecten jacobaeus* (Linnaeus, 1758), the queen scallop *Aequipecten opercularis* (Linnaeus, 1758), and the smooth scallop *Flexopecten glaber* (Linnaeus, 1758). The aims of this study were to (i) obtain data on the reproductive cycle of three scallop species, (ii) identify their growth dynamics, and (iii) describe how environmental conditions impact their growth and reproduction. Through this study, valuable information will be provided that will serve as an important scientific baseline for responsible and sustainable management of these species and future aquaculture attempts.

## Material and methods

### Sample collection

Specimens of three scallop species, *Pecten jacobaeus*, *Aequipecten opercularis*, and *Flexopecten glaber* were collected during the beam trawl fisheries monitoring program in the northern Adriatic area (west coast of the Istria peninsula) (Figure 1). The water depth in this area ranges between 25 m and 35 m. For analysis of the reproductive cycle, ca. 30 specimens of each species were collected at approximate monthly intervals from February 2017 to October 2018. Due to its patchy distribution, *F. glaber* was not collected at each sampling occasion. All specimens were transported to the Institute of Oceanography and Fisheries and processed within 24 h after collection. In the laboratory, soft tissues were removed for the reproductive cycle analysis. Shells from August 2018 were carefully cleaned with tap water, left to air-dry, and stored for later analysis.

### Reproduction

Reproductive cycle analysis was performed applying three complementary approaches: (i) assessment of the gonadosomatic index (GSI), (ii) histological analysis of gonad tissue, and (iii) measuring oocyte size. For the GSI analysis, up to 20 specimens were collected during each sampling occasion. The GSI analysis was performed on a total of 1,097 individuals, i.e., 403 specimens of *P. jacobaeus* (mean shell length ± st. dev. = 100.8 ± 4.4 mm), 395 A. *opercularis* (50.9 ± 3.2 mm) and 299 F. *glaber* (53.6 ± 5.7 mm). Bivalves were opened, and gonads separated from the somatic tissue. After dissection, all parts were placed separately in the pre-weighted porcelain dishes, oven-dried for 48 h at 60°C, and weighted. The GSI was calculated according to Barber and Blake (2006):

$$GSI = \left[ \frac{Gonad\ Weight\ (g)}{Total\ Tissue\ Weight\ (g)} \right] \times 100 \qquad (1)$$

During each sampling occasion, ten additional specimens of each species were collected for the analysis of the gonad histology. Histological analysis was performed on a total of 549 individuals, i.e., 210 P. *jacobaeus*, 200 A. *opercularis* and 139 F. *glaber*. Bivalves were opened, gonad tissue samples dissected, and were then fixed in 10 vol% formaldehyde. Further laboratory analysis included the dehydration at increasing ethanol concentrations, after which the gonad tissue was embedded in paraffin, cut at 5 μm, and stained with hematoxylin and eosin. Gonad development was assessed microscopically (Zeiss Axio Lab A1) by applying the gonad development scale of Arellano-Martínez et al. (2004): undifferentiated, early development, late development, ripe, partially spawned, spent, and reabsorption (Supplemental Figures 1, 2). Furthermore, one photograph of each female gonad slide was taken under 100x magnification (Axiocam105 color camera coupled to the microscope described above), and



**FIGURE 1**
Map showing the sampling area in the N Adriatic Sea.

the diameter of all oocytes with visible nucleus was measured using the Image J software (Schneider et al., 2012).

## Shell growth dynamics

Data on shell growth dynamics were obtained from the analysis of stable oxygen isotope values in shells ($\delta^{18}O_{calcite}$) of the three studied species. Two shells of each species sampled in August 2018 were chosen for light stable isotope analysis ($\delta^{18}O_{calcite}$, $\delta^{13}C_{calcite}$). Left valves were gently brushed to remove most of the epibionts as well as sediment trapped between striae and washed in a 10 vol% acetic acid bath for 30–45 s followed by rinsing in deionized water (Thébault and Chauvaud, 2013). Carbonate samples were collected by milling narrow sample swaths (ca. 2 mm to 4 mm long, 300 µm wide) on the external shell surface by hand under a stereo microscope using a DREMEL Fortiflex drill equipped with a 300 µm tungsten carbide drill bit (Komet/Gebr. Brasseler GmbH and Co. KG, model no. H52104003). The estimated milling depth was ca. 100 µm. Distances between samples were measured on photographs using Image Pro Premier software. Sampling was conducted at relatively high resolution to ensure that at least one complete annual growth cycle was covered in each specimen.

Isotope ratio analyses was performed on a Thermo Finnigan MAT 253 continuous flow – isotope ratio mass spectrometer, equipped with a GasBench II from the University of Mainz, Germany. Samples were measured against an in-house Carrara marble ($\delta^{18}O$ = +2.01 ‰; $\delta^{13}C$ = −1.91 ‰) that was calibrated against NBS-19. Results are expressed as parts per thousand with respect to the Vienna Pee Dee Belemnite standard (‰ V-PDB). Long-term (1.5 years) reproducibility (= accuracy, 1 sigma) of the mass spectrometer is 0.04 ‰ for $\delta^{18}O$ and 0.03 ‰ for $\delta^{13}C$ based on 421 blind measurements of NBS-19. The average 1 sigma internal precision error (eight injections per sample) is 0.04 ‰ for $\delta^{18}O$ and 0.03 ‰ for $\delta^{13}C$. To assess the accuracy (external analytical precision) of the specific samples, we also measured two international reference materials (NBS-19: $\delta^{18}O$ = +1.95 ‰, $\delta^{13}C$ = −2.20 ‰; IAEA 603: $\delta^{18}O$ = +2.46 ‰, $\delta^{13}C$ = −2.37 ‰) within each run. According to these analyses (n = 6), stable carbon and oxygen isotope values were measured accurately to the nearest 0.02 ‰ ($\delta^{13}C$) and 0.04 ‰ ($\delta^{18}O$).

To temporally align the measured $\delta^{18}O_{calcite}$ values, daily modelled seawater salinity and temperature time-series were employed to compute the expected $\delta^{18}O_{calcite}$ chronology. For this purpose, the equation by Friedman and O'Neil (1977) was used:

$$10^3 \ln \alpha_{calcite-water} = 2.78 \left( 10^6 T^{-2} \right) - 2.89 \qquad (2)$$

Stable oxygen isotope data of the water ($\delta^{18}O_{w-SMOW}$) were estimated from modelled salinity data (S) using the equation of Stenni et al. (1995) and data by Peharda et al. (2019):

$$\delta^{18}O_{w-SMOW} = 0.366 \times S - 12.568 \; \left( r^2 = 0.964 \right) \qquad (3)$$

Then, measured $\delta^{18}O_{calcite}$ values were arranged as to obtain the best fit with the expected $\delta^{18}O_{calcite}$ curve. Subsequently, it was possible to reconstruct daily and monthly shell growth rates from the known spatial distances between sample positions and the temporal alignment of the $\delta^{18}O_{calcite}$ data.

## Environmental variables

Information on daily temperature and salinity near the seafloor were extracted from the evaluation results of the Adriatic Sea and Coast (AdriSC) numerical climate model (Denamiel et al., 2019; Denamiel et al., 2021; Pranić et al., 2021) for the 2016–2018 period. The AdriSC evaluation run provided hourly results for the 1987–2018 period at (i) up to 3 km horizontal resolution in the atmosphere with the Weather Research and Forecasting model (WRF; Skamarock et al., 2005) and (ii) up to 1 km horizontal resolution in the ocean with the Regional Ocean Modeling System (ROMS; Shchepetkin and McWilliams, 2009). The performances of the AdriSC coupled atmosphere-ocean models have been thoroughly assessed by Denamiel et al. (2021) and Pranić et al. (2021). They demonstrated that, in general, the AdriSC climate model provides better skills than other regional climate models to reproduce the complex dynamical properties of the Adriatic Sea. Additionally, all AdriSC results can be easily accessed and retrieved via the web interface https://vrtlac.izor.hr/ords/adrisc/interface_form (last access: 2 June 2022; Ivanković et al., 2019; Denamiel et al., 2021).

Concerning the detailed setup of the AdriSC ROMS 1 km simulation used in this study, 35 terrain-following layers with refinements at both surface and bottom provided the vertical structure of the ocean model, whereas the tides were represented with 8 constituents and the fresh-water input was given for 49 rivers along the Adriatic coastline. Finally, for the evaluation period, the AdriSC models were forced with re-analysis results from the 6-hourly ERA-Interim fields at 0.75° resolution (Dee et al., 2011) distributed by the European Centre for Middle-range Forecast (ECMWF) for the atmosphere and the daily MEDSEA dataset at 1/16° resolution (Pinardi et al., 2003) distributed by the Copernicus Marine Environment Monitoring Service (CMEMS) for the ocean.

Hereafter, the AdriSC ROMS 1 km daily bottom results were extracted for the 2016–2018 period at 64 different locations offshore of the western coast of Istria for depths ranging from 26 m to 30 m. The temperature and salinity results of the different locations were then regrouped and averaged.

Remotely sensed chlorophyll data were obtained from the European Space Agency's Ocean Colour – Climate Change Initiative (Sathyendranath et al., 2017). The data were extracted from the www.oceancolour.org/ web portal in the

form of chlorophyll concentration given in mg Chl *a* m$^{-3}$. Technical specifications and details concerning the data sets are available *via* climate.esa.int/en/projects/ocean-colour/key-documents/. The data products are merged from SeaWiFS, MODIS, MERIS and VIIRS satellite sensors. The entire data set spans a time frame from September 1977 to December 2019. We limited our analysis from February 2017 to October 2018 and used version 4.2 monthly data for the following region: NW 45°25'45.89"N, 13°13'05.03"E, NE 45°25'40.34"N, 13° 29'29.21"E, SE 45°05'59.19"N, 13°35'31.82"E, SW 45° 06'12.86"N 13°18'14.73"E. The data pixels that approximated this region were the best chosen and averaged spatially for each month. An application of a prior version of this data set to the Adriatic can be found in Markulin et al. (2020).

Spearman's rank correlation was used to determine the degree of association between mean gonadosomatic indices, mean growth rates, temperature, salinity, and chlorophyll *a*. For the correlation between GSIs and temperature, 30-day averages prior to the sampling day were computed. For the comparison with bulk phytoplankton biomass, monthly Chl-*a* averages (the month before the respective sampling date) were used.

# Results

## Reproduction

### Gonado-somatic indices

GSI values exhibited seasonal and interspecies variations. In both studied years, the highest mean GSI values for *P. jacobaeus* were recorded during late summer and early fall (Figure 2A). In 2017, the maximum value was recorded at the end of September (18.0 ± 5.1). Afterward, a sharp decrease was observed until the end of November (4.0 ± 2.1). The lowest GSIs in 2017 were recorded between May and mid-July (1.8 ± 0.6 to 3.0 ± 1.8), while during the same time interval in 2018, GSI values were higher. During winter and early spring of 2018, GSI increased until March and April (10.5 ± 3.7 and 10.5 ± 4.3, respectively), followed by a decrease until July, when minimal values were recorded (1.5 ± 0.9). Following the GSI results, *P. jacobaeus* could have reproduced twice per year.

*A. opercularis* showed maximum GSI values in late winter/ spring and lowest during late summer. However, interannual differences were observed (Figure 2B; i.e., maximum GSI values lasted longer in 2018 compared to 2017). In 2018, higher values were recorded between January and late May (between 9.7 ± 1.8 and 12.6 ± 3.4). Values started to decrease in late spring, reaching a minimum during late summer (between 2.3 ± 0.8 and 2.4 ± 0.9). In 2017, the highest mean GSI value was recorded in mid-March (13.7 ± 4.7), while lower values were recorded at the beginning of May (4.6 ± 1.1), and values continued to decrease during summer, reaching minimal levels in the late summer and early fall (between 2.3 ± 1.1 and 2.7 ± 1.6). Although *F. glaber* was not collected on all

sampling occasions, from the obtained GSI, it is evident that this species had higher GSI in the late spring and early summer during both years (2017: 17.1 ± 9.9; 2018: 25.4 ± 6.3), clearly indicating a summer spawning peak (Figure 2C). GSI values decreased in late summer and remained low during the rest of the survey period (fall/winter). GSI results suggest that *A. opercularis* and *F. glaber* had one reproductive cycle per year.

Only GSI indices of *A. opercularis* revealed a statistically significant correlation with environmental parameters. While for the other two species, a correlation between GSI and environmental parameters was not found. GSI of *A. opercularis* correlated positively with chlorophyll-*a* concentration (r = 0.70, p< 0.001) but negatively with temperature (r = -0.86, p< 0.001).

## Histological analysis of gonad tissue

According to such analyses, *P. jacobaeus* may have had two reproduction peaks during the year without a gonad resting period (Figure 3A). At the beginning of the sampling in winter 2017, *P. jacobaeus* was in the spawning phase with a few ripe individuals. First individuals in early gametogenesis were found in the late spring of 2017, ripening until late summer, and gamete release started in the early fall of 2017. It is interesting to note that ripe gametes were still present in high numbers during the fall spawning peak, while developing previtellogenic oocytes were also abundant in the same follicles. These oocytes continued to mature during winter so that another spawning event occurred in spring 2018. During this maturation event, *P. jacobaeus* did not show a clear early development phase of gametogenesis that typically occurs as the first phase in gametogenesis after spawning. After spawning in spring of 2018, intensive gametogenic activity started immediately, and the first individuals in the early active phase were recorded at the beginning of summer 2018, while ripe individuals were recorded from mid-summer onward. Although spawning females were not recorded on the last sampling occasion in October 2018, spawning males were present among the studied specimens. Therefore, it could be assumed that fall spawning commenced in the months following this study.

The histological analysis confirmed that *A. opercularis* had one reproductive cycle per year with minor interannual differences (Figure 3B). In 2017, most studied specimens were ripe during the winter, followed by a prolonged gamete release interval from spring to mid-summer. The short gonad resting period was recorded in mid-summer, followed by a period of intensive gametogenic activity. The first ripe individuals were recorded in late fall of 2017. In 2018, unlike the previous year, most studied specimens were ripe by late spring, when the prolonged spawning season started. In 2018, the gonad resting period was not as pronounced as in 2017.

Although it was not feasible to collected *F. glaber* specimens continuously during the study, histological data indicated that this species had one reproductive cycle per year with a prolonged gonad resting period (Figure 3C). Gametogenesis started during
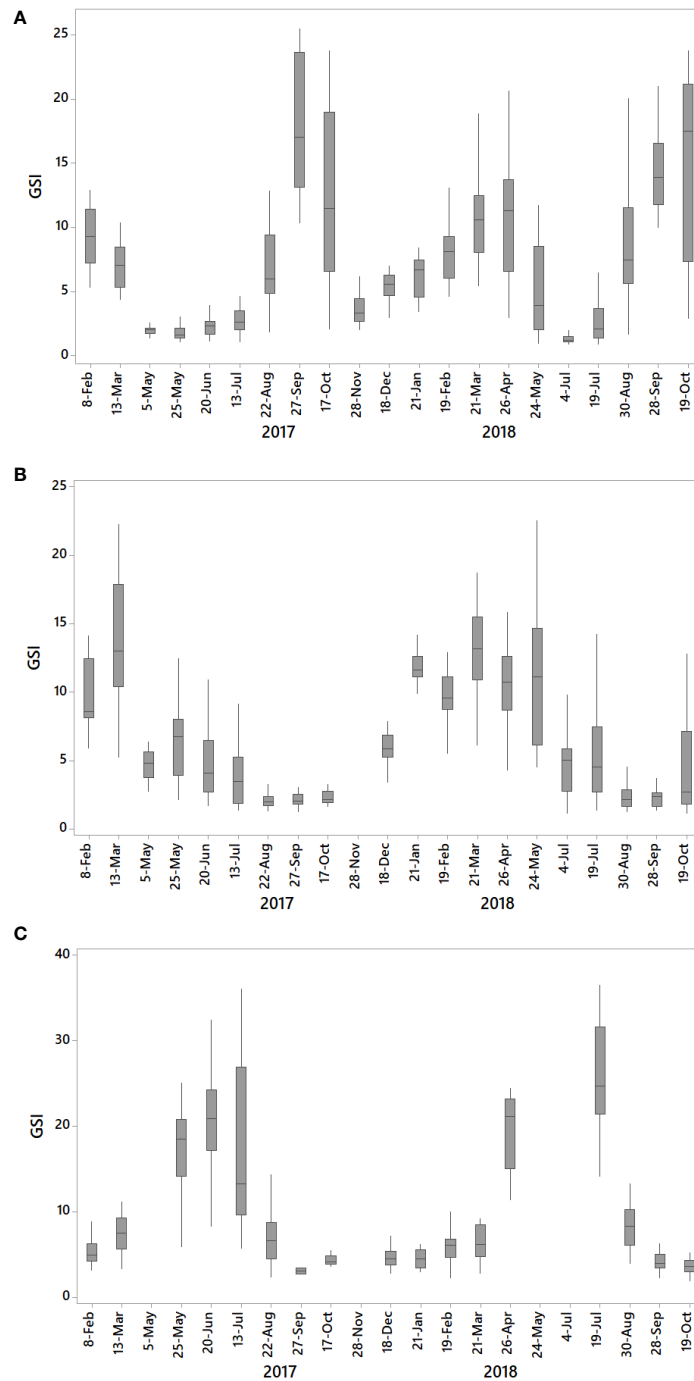
**FIGURE 2**
Gonadosomatic indices (GSI) during the studied time interval for **(A)** *Pecten jacobaeus*, **(B)** *Aequipecten opercularis*, and **(C)** *Flexopecten glaber*.

the late fall/early winter and reached maturation in spring. Spawning occurred during the summer.

During the survey period, all three studied species had a small portion of individuals whose ripe female gametes underwent reabsorption, in some cases representing pre-

spawning atresia (Supplemental Figures 1F, L and S). Among the studied species, the highest occurrence of reabsorption was noted in *P. jacobaeus* in June 2018. Although gonad reabsorption was not reported in the male individuals this could be due to the more challenging identification.

Monthly variation in the frequency of different gametogenic stages of **(A)** females and **(B)** males of *Pecten jacobaeus*, **(C)** females and **(D)** males of *Aequipecten opercularis*, and **(E)** females and **(F)** males of *Flexopecten glaber*. ED, early development; LD, late development; R, ripe; PS, partially spawning; S, spent.
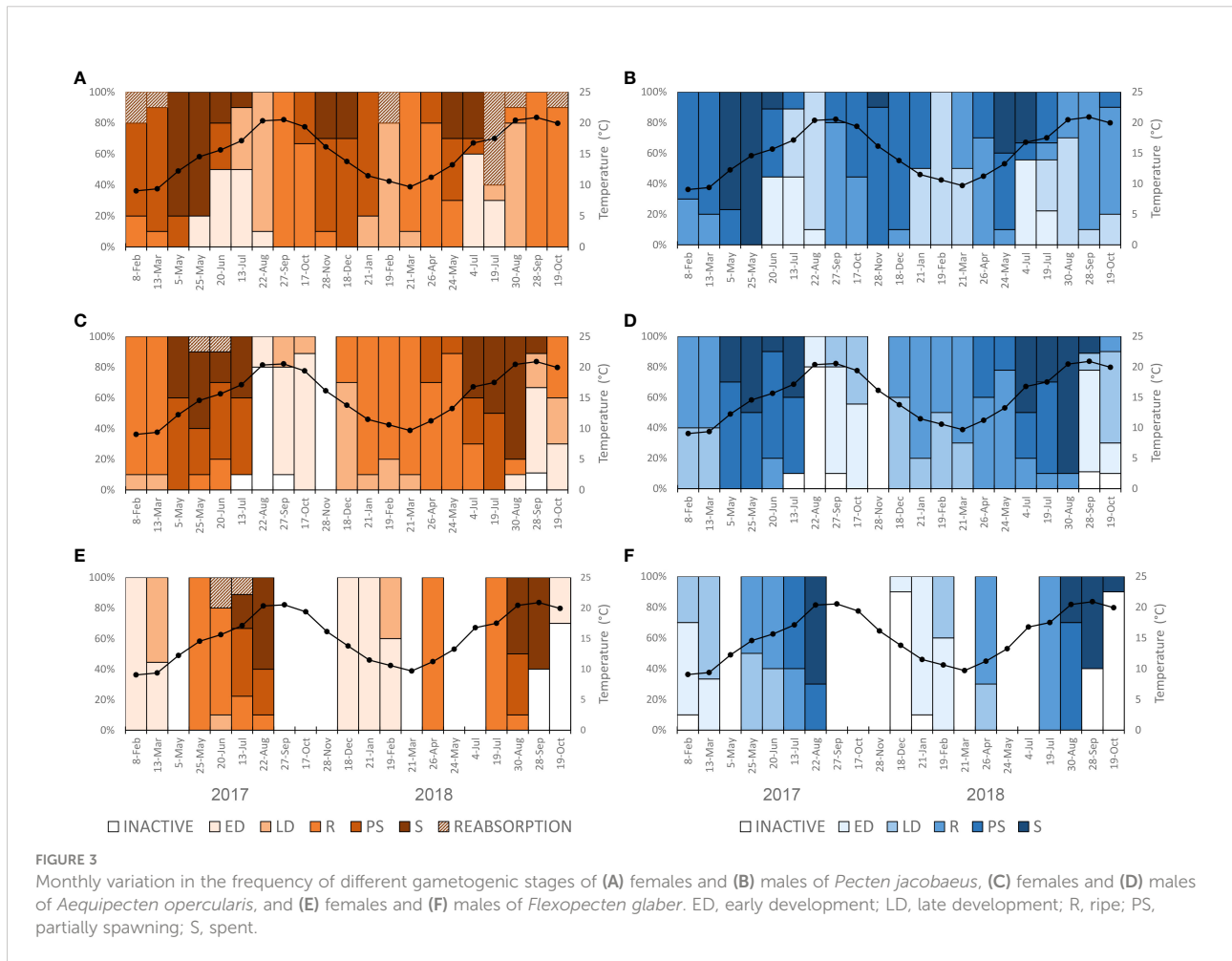
## Oocyte size

Changes in the size distribution of *P. jacobaeus* oocytes during the survey period are depicted in Supplemental Figure 3. During 2017, oocyte sizes increased from mid-spring/early summer (11.7 ± 14.3 µm; June 2017) to late summer/early fall (65.2 ± 12.7 µm; September 2017). Afterward, larger oocytes were still present, but a fraction of the smaller oocytes increased, forming a bimodal distribution. While oocytes started ripening, their diameter reached the second peak in spring 2018. Smaller oocytes dominated in mid-summer (12.1 ± 11.3 µm; beginning of July 2018), and their diameter increased in the following period.

During winter of 2017, the oocyte diameter of *A. opercularis* showed a bimodal distribution indicating both small and large oocytes were present (Supplemental Figure 4). Afterward, the average oocyte diameter decreased and reached a minimum during late summer (11.8 ± 9.6 µm; September 2017). During fall of 2017 and winter of 2018, oocyte size started to increase, and maximal average oocyte diameter was recorded in spring of 2018 (60.1 ± 11.3 µm; May 2018), followed by a decrease reaching

minimal values in the late summer of 2018 (12.7 ± 11.5 µm; September 2018).

*F. glaber* was not sampled during the entire survey period. Detailed patterns of oocyte growth are not available, but a similar pattern was observed during both sampling years (Supplemental Figure 5). Smaller oocytes were dominant during fall and winter, with minimal average size recorded in December 2017 (7.7 ± 2.13 µm). Oocytes size increased during spring reaching the maximal size in the late spring/early summer period. The maximum oocytes size in 2017 was recorded in June (56.5 ± 15.9 µm), whereas in 2018 it occurred in July (57.2 ± 15.4 µm), after which average oocyte sizes decreased.

## Shell growth dynamics

A total of 369 stable isotope samples from six shells belonging to three different scallop species were analyzed (Table 1). Mean distances between milling steps were 0.57 ± 0.14 mm in the case of *P. jacobaeus*, 0.46 ± 0.09 mm for *A. opercularis*, and 0.43 ± 0.10 mm for *F. glaber*. The $\delta^{18}O_{calcite}$

amplitudes were relatively similar for *Pecten jacobaeus* (2.77‰ and 2.78‰) and *F. glaber* (2.70‰ and 2.43‰) shells. Lowest $\delta^{18}O_{calcite}$ amplitudes were observed in *A. opercularis* (2.38‰ and 2.00‰). All $\delta^{18}O_{calcite}$ values were positive and ranged from 0.28‰ (*P. jacobaeus*, PJ1) to 3.79‰ (*F. glaber*, FG1). For *F. glaber*, all $\delta^{18}O_{calcite}$ values were higher than 1‰ (Supplemental Figure 6). $\Delta^{13}C_{calcite}$ amplitudes varied between specimens and species and ranged from 1.01‰ (*A. opercularis*, AO1) to 1.58‰ (*F. glaber*, FG1).

Temporal alignment of the $\delta^{18}O_{calcite}$ values clearly illustrated variations in growth seasonality of the three analyzed species (Figures 4, 5). *Pecten jacobaeus* deposited shell material during most of the year, except when seawater temperatures exceeded ca. 20°C. *Aequipecten opercularis* grew mainly during the warm part of the year. A growth slowdown/cessation occurred during the colder part of the year, between January and March (i.e., when seawater temperatures dropped below ca. 11°C). The third species, *F. Glaber*, revealed a pronounced seasonal pattern with a growth slowdown/cessation when seawater temperatures increased above ca. 18°C (August–October). Significant shell deposition took place during the cold period. Seasonality of growth is clear in cumulative growth curves (Supplementary Figure 7).

Studied portions of *P. jacobaeus* were formed between the end of age three and five, while those of the two other species were precipitated during the end of age one and three. *P. jacobaeus* attained highest shell formation rates of 0.068 mm and 0.106 mm day$^{-1}$ in PJ1 and PJ2, respectively (Figure 5). With up to 0.250 mm day$^{-1}$ (specimen AO1) and 0.277 mm day$^{-1}$ (AO2), *A. opercularis* grew much faster than *P. jacobaeus*. The fastest shell growth rates were obtained for *F. glaber*, reaching 0.283 mm day$^{-1}$ for FG1 and 0.301 mm day$^{-1}$ for FG2. A statistically significant positive correlation was found between mean monthly growth rate and chlorophyll-*a* concentration for *P. jacobaeus* ($p < 0.001$, $R = 0.67$) and *F. glaber* ($p < 0.001$, $R = 0.73$).

## Environmental variables

Modelled daily temperature ranged from 7.6°C to 22.8°C, with temperatures below 10°C prevailing between mid-January and mid-March 2017 as well as late February to mid-March 2018. The beginning of 2016 was the warmest of the three studied years, with seawater temperatures of ca. 12°C. Highest temperatures above 20°C were characteristic for August and September and were rather similar between all years. Salinity ranged from 38.1 to 38.7, with a certain degree of periodicity. Lowest values were noted for summer months, while highest values were observed early in the year. Summer 2017 was characterized by higher summer salinity in comparison to the previous and following years (Supplementary Figure 8).

The study area was characterized by two chlorophyll-*a* peaks, one more expressed in fall and the other in spring (Supplementary Figure 9). Average monthly chlorophyll-*a* concentration during the studied time interval ranged from 0.33 mg m$^{-3}$ to 1.00 mg m$^{-3}$. In 2017, the lowest monthly values were recorded during the summer (i.e., July to September from 0.45 ± 0.08 mg m$^{-3}$ to 0.47 ± 0.08 mg m$^{-3}$), while the highest monthly value was recorded in fall (1.00 ± 0.11 mg m$^{-3}$). The highest spring values equalled 0.74 ± 0.25 mg m$^{-3}$ and 0.73 ± 0.17 mg m$^{-3}$, recorded in April and May, respectively. The same pattern was observed in 2018, with a chlorophyll-a minimum during the summer (July and August: 0.34 ± 0.11 mg m$^{-3}$ and 0.33 ± 0.15 mg m$^{-3}$, respectively) and maximum in fall (November: 1.29 ± 0.14 mg m$^{-3}$). The spring chlorophyll-*a* peak was recorded in April (0.89 ± 0.20 mg m$^{-3}$).

## Discussion

This study used a multi-species approach to analyse reproductive and growth strategies of three commercially important scallop species, namely, *P. jacobaeus*, *A. opercularis*,

TABLE 1 Overview of studied bivalves and descriptive statistics for $\delta^{18}O_{calcite}$ and $\delta^{13}C_{calcite}$.

| Species | ID | Shell L and H (mm) | N | $\delta^{18}O_{calcite}$ (‰) range (amplitude) | $\delta^{13}C_{calcite}$ (‰) range (amplitude) | Length of sampled portion (mm) |
|---|---|---|---|---|---|---|
| *Pecten jacobaeus* | PJ1 | 104.1 85.0 | 38 | +0.28 — +3.05 (2.77) | -0.91 — +0.11 (1.02) | 20.6 |
| | PJ2 | 110.6 85.0 | 41 | +0.43 — +3.21 (2.78) | -1.32 — -0.02 (1.31) | 24.6 |
| *Aequipecten opercularis* | AO1 | 56.5 55.6 | 58 | +0.21 — +2.59 (2.38) | -1.77 — -0.75 (1.01) | 27.3 |
| | AO2 | 55.4 54.0 | 69 | +0.43 — +2.43 (2.00) | -2.22 — -0.68 (1.55) | 30.4 |
| *Flexopecten glaber* | FG1 | 60.0 58.9 | 74 | +1.09 — +3.79 (2.70) | -1.10 — +0.47 (1.58) | 36.1 |
| | FG2 | 57.8 55.4 | 89 | +1.09 — +3.51 (2.43) | -1.10 — +0.28 (1.38) | 32.9 |

Isotope sampling was performed along the axis of maximum growth and accordingly the milling distance values came from that axis. L, shell length; H, shell height.
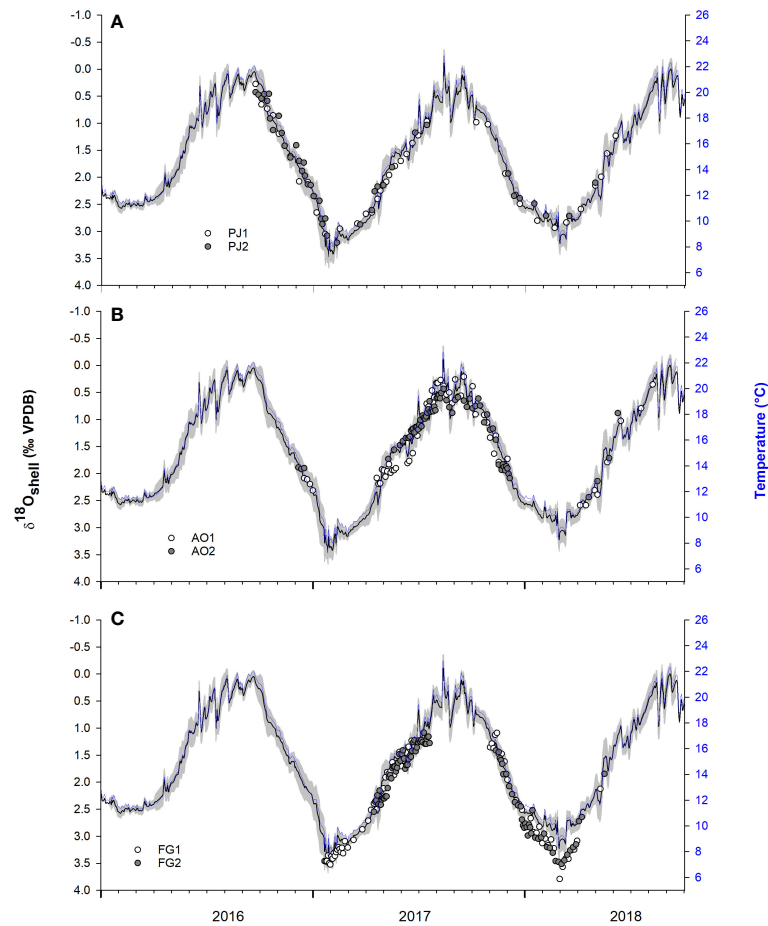
**FIGURE 4**
Predicted shell oxygen isotope values (black lines; grey area represents the 30 day running 1σ uncertainty) computed from water temperature (AdriSC ROMS model) and δ$^{18}$O$_{water}$ values computed from salinity (AdriSC ROMS model) using the palaeothermometry equation by Friedman' O'Neil (1977). White and grey circles represent temporally aligned δ$^{18}$O$_{calcite}$ values of **(A)** *Pecten jacobaeus* (PJ1, PJ2), **(B)** *Aequipecten opercularis* (AO1, AO2), and **(C)** *Flexopecten glaber* (FG1, FG2). Note, scale on y$_1$-axes is reversed. Modelled daily sea surface temperature is depicted in dark blue on y$_2$-axis.

and *F. glaber*. These three related species were comparatively analyzed and clearly indicate diverse strategies employed. Specimens analyzed inhabit the same location and were exposed to the same environmental conditions. Multi-species comparisons are relatively rare and can provide valuable insights into the ecology of the individual species.

## Reproduction

The reproduction cycle is a complex process that is affected by various exogenous and endogenous factors as well as interactions between them (Gosling, 2015). Temperature and food availability have been identified as main external forcings affecting the reproductive cycle in sessile animals including bivalves (e.g., Martínez et al., 2000; Bernard et al., 2011;

Gosling, 2015). Despite experiencing the exact same environmental condition, the three studied (hermaphroditic) species belonging to the same family (Pectinidae) exhibited different reproductive cycle patterns. Our results were confirmed by applying three complementary methods being (i) gonadosomatic indices, (ii) histological analysis of gonad tissue, and (iii) oocyte size. Together this approach enabled a robust analysis.

Among the three investigated species, only *P. jacobaeus* showed two reproductive peaks in one year, one strong peak in fall and a weaker in spring. Previous studies on the reproductive cycle of *P. jacobaeus* are rare. The only available year-round studies on the reproduction of this species were done by Marguš and Teskeredžić (2005) in the central part of the eastern Adriatic Sea (the Prokljan Lake, Krka River estuary) and Castagnolo (1991) in the north-west part of the Adriatic Sea.
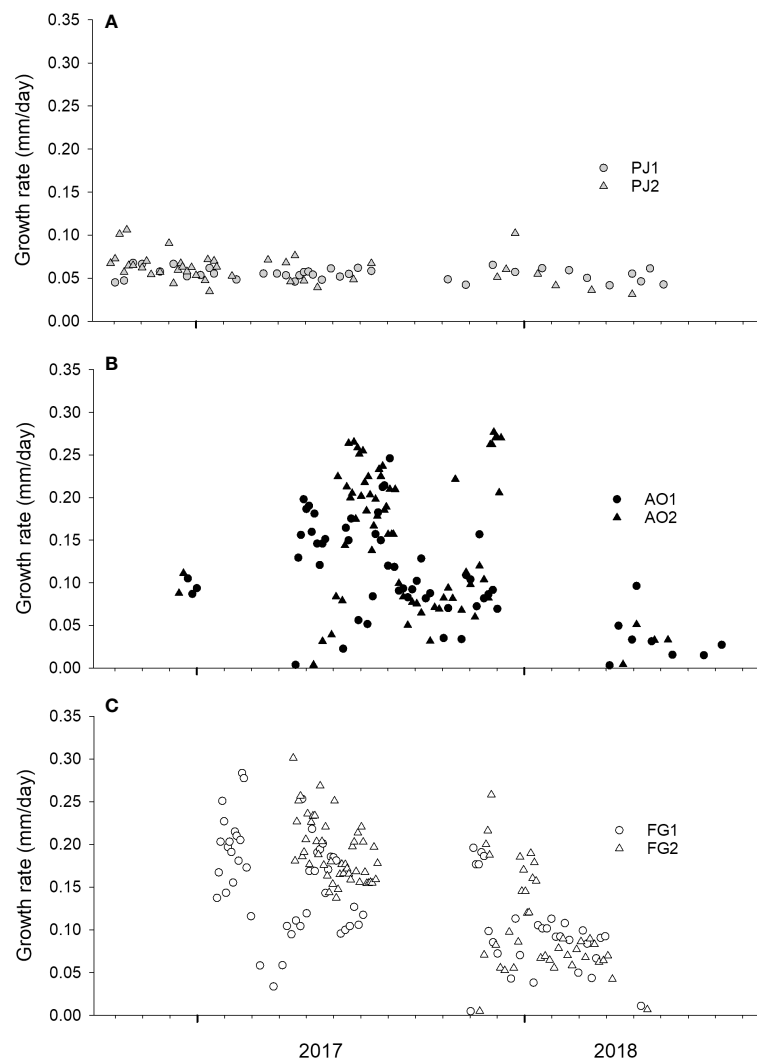
**FIGURE 5**
Estimated daily growth rates of **(A)** *Pecten jacobaeus* (PJ1, PJ2), **(B)** *Aequipecten opercularis* (AO1, AO2), and **(C)** *Flexopecten glaber* (FG1, FG2). Results are based on spatial distances between milled samples and $\delta^{18}$O-based temporal alignment of the samples (see Figure 4).

Marguš and Teskeredžić (2005) analyzed variations in gonad index and reported only one reproductive peak per year occurring in late winter/early spring, while during the rest of the year, GSI remained low. Interestingly, during late summer/ early fall, when GSI values in the present study were at a maximum, *P. jacobaeus* from the Krka estuary had the lowest GSI values. A recent study by Topić Popović et al. (2020), conducted in the same area where the current study was performed, also recorded the highest GSI values in fall. Unfortunately, in their study, the authors only performed seasonal sampling, so it is not possible to determine if there was more than one reproductive peak. Based on the histological analysis of gonad tissue, Castagnolo (1991) even reported three spawning events for *P. jacobaeus* in May, August, and

December. Spatial differences in the reproductive cycle were also observed for *P. maximus* where two populations in Britany expressed different reproductive traits. The population from St. Brieuc Bay showed the first spawning event in early July, while a second spawning period lasted until the end of August. In contrast, *P. maximus* population from Bay of Brest spawned between May and September (Paulet et al., 1988). Similarly, differences in the reproductive cycle were recorded at five locations in Norway. Based on the reproductive patterns, Magnesen and Christophersen (2008) argued that the studied *P. maximus* belonged to three different populations. Observed differences in the reproductive pattern probably reflect a different environment that the bivalves inhabited and/or an adaptation of this species to the different environment.

Considering observed variability of the reproductive cycle, knowledge about reproductive biology is crucial for a sustainable shellfisheries management in areas where *P. jacobaeus* is intensively exploited such as the northern Adriatic Sea. This study provides the first comprehensive data set about the reproductive biology of *P. jacobaeus* in this region and therefore represents a valuable scientific base for the sustainable management of this species.

Knowledge about the reproduction of the other two investigated species, *A. opercularis* and *F. glaber*, is also scarce. Considering their growing commercial value, due to the depletion of the *P. jacobaeus* stocks, data from the present study are extremely valuable in the light of future sustainable management strategies. According to the results herein generated from specimens of the North Adriatic Sea, both species showed one pronounced reproductive cycle per year. In *F. glaber*, the spawning season started in summer, while it occurred a few months earlier (spring) in *A. opercularis*. Available studies on the reproductive cycle of *A. opercularis* were mainly done in the NE Atlantic and results differ from our findings. Román et al. (1996) pointed out that *A. opercularis* from Galicia, NW Spain, had two spawning peaks, one in June–July and a second in September. As their study was only based on GSI values, the authors suggested that this could also be due to the resorption, common phenomena in scallop species. Taylor and Venn (1979) found that *A. opercularis* spawns during summer/fall in the Clyde Sea, Scotland. Our data also differ from results of the only available study in the Adriatic Sea by Castagnolo (1991). These authors suggested that spawning in the NW Adriatic Sea occurs year-round, with prominent peaks in January, May, August, and September. Such differences could be driven by local environmental conditions. Spawning could also vary between years. Furthermore, differences in analytical methods could have caused the observed differences in spawning.

Data obtained for *F. glaber* are in accordance with a recent study by Marčeta et al. (2016) from the NW Adriatic Sea. As in our study, they observed a major spawning event between July and September, but also a minor spawning event between April and May, which was not present in our data set. According to a recent spat settlement survey in the Ionian Sea (Tsotsios et al., 2016), the spat settlement maximum occurred in July suggesting the main spawning event occurred approximately in June (i.e., one month prior to that in the northern Adriatic). Differences in reproductive strategy in different populations of the same species were previously described and put in relation to different nutritional, environmental conditions, and/or geographical locations (Magnesen and Christophersen, 2008; Duncan et al., 2016). Furthermore, Mackie and Ansell (1993) suggested differences in reproductive physiology could indicate the existence of partially genetically separated stocks. However, to confirm this, more detailed studies are required.

Oocyte atresia, autolysis process of structurally normal oocytes (Beninger, 2017), was recorded in all three studied species and were most pronounced in *P. jacobaeus*. This phenomenon was previously described for many bivalve species, including scallops (for review see Beninger, 2017). Le Pennec et al. (1991) recorded oocyte atresia in *P. maximus* throughout the year, mostly during the late vitellogenesis, stage when many large yolk inclusions are present in the oocytes. However, when interpreting the reproductive cycle, we need to be aware of two differently timed types of oocyte atresia: (i) post-spawning atresia that occurs at the end of the reproductive period when residual oocytes degenerated in the gonads and (ii) pre-spawning atresia that occurs prior to spawning events (Le Pennec et al., 1991; Beninger, 2017). According to Beninger (2017), pre-spawning atresia are more common than it is reported and, if not recognized, could result in misinterpretation of the reproductive cycle. Some authors connected pre-spawning atresia and environmental conditions (e.g., low or high temperature). However, physiological regulatory mechanisms that could lead to atresia cannot be excluded (Dutertre et al., 2009; Camacho-Mondragón et al., 2015; Beninger, 2017 and references therein). Considering pre-spawning atresia in studied scallop species were found during different seasons, future research is needed to untangle its causes.

## Growth

According to $\delta^{18}O_{calcite}$-based temporal alignment of the shell record, the three studied scallop species exhibited different seasonal growth dynamics. Although this analysis was performed on a small number of individuals, it was conducted at high-resolution on specimens collected from the same sampling site, thereby enabling comparative analysis. *P. jacobaeus* and *F. glaber* slowed down growth when seawater temperature was elevated (>20°C and 18°C, respectively), while *A. opercularis* slowed down the biomineralization rate during the colder part of the year (< 11°C). Besides temperature, shell growth of *P. jacobaeus* and *F. glaber* was related to chlorophyll-*a* concentration, suggesting food availability as one of the main factors influencing shell formation rate of these species.

As previously reported by Peharda et al. (2019), the slowdown and/or cessation of shell growth in *P. jacobaeus* occurs during the warmest part of the year. The same authors also suggested that annual growth lines in *P. jacobaeus* are formed between September and November, pointing toward other factors affecting growth besides temperature. In our study, *P. jacobaeus* growth slowdown/cessation took place between mid-summer and mid-fall with slight inter-annual differences. This period corresponded with a sharp increase in GSI values indicating increased gametogenesis activity (Figure 6A), suggesting *P. jacobaeus* transferred energy from

shell growth to reproduction during this time of the year. Peharda et al. (2019) hypothesized that energy is redirected to growth when spawning is over. This pattern was also observed in our study during the spring 2017. However, during winter and spring of 2018, both growth rates and GSI values were high, indicating that *P. jacobaeus* had enough energy to sustain shell growth and gametogenesis activity. Prior to the period of intensive gametogenesis and shell growth, high chlorophyll-*a* concentrations were recorded, which could trigger such a physiological response.

Observed seasonal growth dynamics of *P. jacobaeus* in the Adriatic Sea differs notably from that of the sister species, *P. maximus*. According to Chauvaud et al. (2005), in the Bay of Brest, (NW France), *P. maximus* deposits shell material mainly between April and October and has a pronounced winter growth stop or slow down. Summer seawater temperatures in the Bay of Brest did not exceed ca. 17°C (see Figure 3, Chauvaud et al., 2005), which is several degrees lower than respective temperatures in the NE Adriatic Sea. Shell deposition during the warm part of the year and the winter growth stop were also identified in *P. maximus* from other locations in the E Atlantic Ocean (see Chauvaud et al., 2012).

Although *A. opercularis* inhabits the same environment as *P. jacobaeus*, our analysis showed that it has different growth dynamics, with the most intensive shell growth during the warmer part of the year. In 2017, growth commenced in April



FIGURE 6
Average monthly growth rates and gonadosomatic index values (GSI) during the studied time interval for **(A)** *Pecten jacobaeus,* **(B)** *Aequipecten opercularis,* and **(C)** *Flexopecten glaber.*
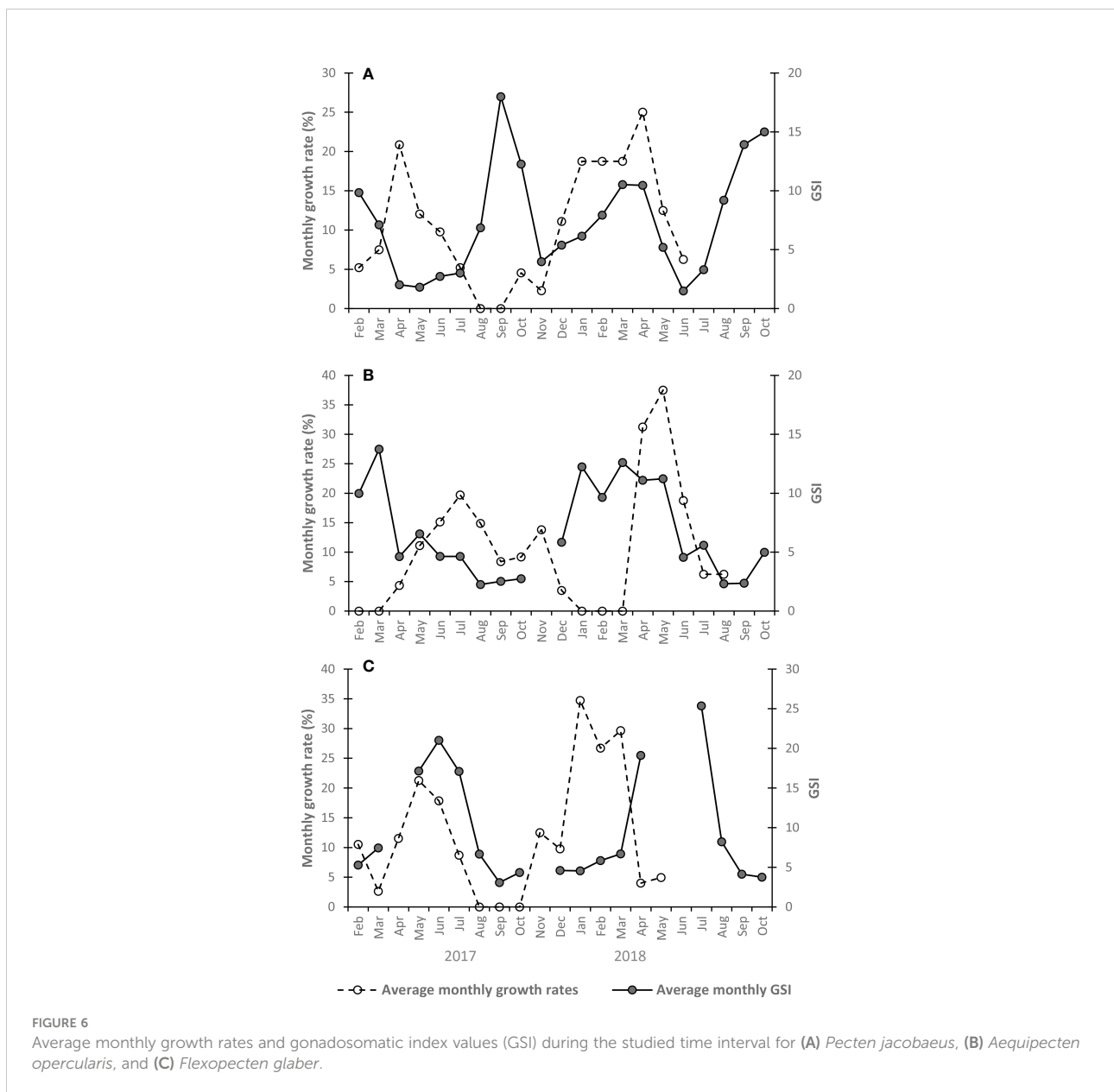
after the main spawning event. Shell growth increased during the prolonged spawning period and started to decrease with the beginning of gametogenesis (Figure 6B), indicating that *A. opercularis* redirected most energy to the growth when spawning was over. A slight increase in growth rate in November might be triggered by the observed chlorophyll-*a* increase. At the time when GSI reached the maximum, shell growth cessation occurred in mostly ripe individuals. Shell growth continued immediately after the first spawning event in April 2018, probably triggered by increasing sweater temperature and chlorophyll-*a* concentration. The δ¹⁸O data of *A. opercularis* shells from the southern North Sea and the English Channel also confirmed growth cessation during the winter associated with the formation of annual growth lines (Hickson et al., 1999; Heilmayer et al., 2004). Heilmayer et al. (2004) indicated that rings are formed during the lowest temperatures and low primary production in the English Channel.

To the best of our knowledge, the present study provides the first data on seasonal growth of *F. glaber*. Although some inter-annual differences were visible in the growth rates, *F. glaber* grows faster during the colder part of the year, while its growth slows down or completely stops during summer and early fall. Furthermore, the correlation between growth rate and chlorophyll-*a* concentration led to the conclusion that food availability directly influences shell growth. Scarce information on the reproductive cycle does not allow for a detailed comparison of the growth dynamics and energetic investment into reproduction (Figure 6C).

Daily growth rates obtained in this study contribute to the understanding of the growth dynamics of commercially important scallops. According to a recent study by Thébault et al. (2021), daily shell growth rates of *Pecten maximus* ranged from 0.05 mm day⁻¹ in late February representing the beginning of the main growing season, to ca. 0.25 mm day⁻¹ during the summer months. These values were obtained from shells after their first annual ring was formed, which corresponds to an ontogenetically earlier period than the data collected in the present study (ca. 0.10 mm day⁻¹). A significant decrease in daily growth rate of *P. maximus* with increasing age was clearly identified by Chauvaud et al. (2012) that looked at variations along a latitudinal gradient. In that study, broadest daily growth increments of as much ca. 0.30 mm were noted during early ontogeny and only at several locations, which were characterized by a relatively short growing season (up to 130 days). At some locations, daily growth rates significantly decreased to ca. 0.10 mm per day between age three and five, a finding that agreed with our results.

In the present study, daily growth rates for *A. opercularis* and *F. glaber* exceeded 0.10 mm day⁻¹ for much of the main growing season. Maximum daily growth rates for both species attained ca. 0.30 mm day⁻¹, which corresponds to values presented above for *P. maximus*. Studies on daily growth of *A. opercularis* and *F. glaber* are still rather limited. Román et al. (1999) analyzed growth of *A. opercularis* under aquaculture conditions in Ría de Arosa (Galicia,

NW Spain) and obtained average growth rates of 0.11 mm day⁻¹, based on specimens with an initial height of 22 mm. Lowest growth rates occurred during the colder part of the year (January to April), which is consistent with the growth slowdown/cessation observed in *A. opercularis* in the present study. Marčela et al. (2016) experimentally cultured *F. glaber* at a coastal site in the NW Adriatic Sea (Porto Caleri, Italy) from January to August and determined an average growth rate of 0.078 mm day⁻¹. They used specimens with an initial height of ca. 18 mm, and the study lasted for only seven months. Spatial variations in growth rates of *P. maximus* were mentioned by Chauvaud et al. (2012) pointing out the need to conduct a wider study of shell growth rates in *A. opercularis* and *F. glaber*. Ideally, such an undertaking includes a broad spectrum of habitats with different environmental conditions to obtain a more complete insight into the growth potential of these commercially important species.

## Conclusions

This study contains results on reproduction and growth strategies of three commercially important scallop species including *P. jacobaeus*, *A. opercularis*, and *F. glaber*, collected from their natural habitat in the NE Adriatic Sea. Although life strategies are flexible and can differ at other locations in the Mediterranean Sea, this multi-species approach enabled a comparative analysis and provided meaningful insights into variations of reproductive strategies. Late summer and early fall have been identified as the main spawning period for *P. jacobaeus*, complemented by another, smaller spawning event in spring. The reproductive cycle of *A. opercularis* was characterized by winter spawning, while *F. glaber* released gametes during early to mid-summer. Seasonal growth dynamics also varied between species. *Pecten jacobaeus* and *F. glaber* slowed down growth during periods of elevated seawater temperatures, wheras *A. opercularis* slowed down growth during the cold season.

## Data availability statement

The raw data supporting the conclusions of this article will be made available by the authors, without undue reservation.

## Author contributions

DE-B designed experiment related to reproduction, conducted fieldwork, analyzed data, and wrote manuscript. MP obtained funding, designed experiment related to growth, analyzed data, and wrote manuscript. BS designed experiment related to stable isotopes and growth, analyzed data, wrote manuscript. HU milling of carbonate material, help with data analysis, writing and revision of the manuscript. NV obtained

funding, organized fieldwork, help with writing and revision of the manuscript. KM milling of carbonate material, help with writing and revision of the manuscript. IR preparation of histological slides, help with writing and revision of the manuscript. CD numerical ocean model data, help with writing and revision of the manuscript. ŽK analysis of remotely sensed chlorophyll data, help with writing and revision of the manuscript. All authors gave final approval of the version to be published.

## Funding

## Acknowledgments

## Conflict of interest

The authors declare that the research was conducted in the absence of any commercial or financial relationships that could be construed as a potential conflict of interest.

## Publisher's note

All claims expressed in this article are solely those of the authors and do not necessarily represent those of their affiliated organizations, or those of the publisher, the editors and the reviewers. Any product that may be evaluated in this article, or claim that may be made by its manufacturer, is not guaranteed or endorsed by the publisher.

## Supplementary material

The Supplementary Material for this article can be found online at: https://www.frontiersin.org/articles/10.3389/fmars.2022.992042/full#supplementary-material

## References

Andersen, S., Christophersen, G., and Magnesen, T. (2011). Spat production of the great scallop (*Pecten maximus*): A roller coaster. *Can. J. Zool.* 89, 579–598. doi: 10.1139/z11-035

Arellano-Martínez, M., Ceballos-Vázquez, B., Villalejo, M., Garcia Dominguez, F., Elorduy-Garay, J. F., Esliman-Salgado, A., et al. (2004). Reproduction of the lion's paw scallop *Nodipecten subnodosus Sowerby* 1835 (Bivalvia: Pectinidae) from Laguna ojo de liebre, B.C.S., México. *J. Shellfish. Res.* 23, 723–729.

Armelloni, E. N., Scanu, M., Masnadi, F., Coro, G., Angelini, S., and Scarcella, G. (2021). Data poor approach for the assessment of the main target species of rapido trawl fishery in Adriatic Sea. *Front. Mar. Sci.* 8. doi: 10.3389/fmars.2021.552076

Barber, B. J., and Blake., N. J. (2006). "Reproductive physiology," in *Scallops: Biology, ecology and aquaculture*. Eds. S. E. Shumway and G. J. Parsons (Amsterdam: Elsevier), 357–416.

Beninger, P. G. (2017). Caveat observator: The many faces of pre-spawning atresia in marine bivalve reproductive cycles. *Mar. Biol.* 164, 163. doi: 10.1007/s00227-017-3194-x

Bernard, I., de Kermoysan, G., and Pouvreau, S. (2011). Effect of phytoplankton and temperature on the reproduction of the pacific oyster *Crassostrea gigas*: Investigation through DEB theory. *J. Sea. Res.* 66, 349–360. doi: 10.1016/j.seares.2011.07.009

Camacho-Mondragón, M. A., Ceballos-Vázquez, B. P., Uría-Galicia, E., López-Villegas, E. O., Pipe, R., and Arellano-Martínez, M. (2015). Ultrastructural and histological study of oogenesis and oocyte degeneration in the penshell *Atrina maura* (Bivalvia: Pinnidae). *Malacologia* 59, 1–12. doi: 10.4002/040.059.0102

Castagnolo, L. (1991). La pesca e la riproduzione di *Pecten jacobaeus* l. e di *Aequipecten opercularis* (L.) nell'Alto adriatico. *Boll. Malacologico.* 27, 39–48.

Cetinić, P., and Soldo, A. (1999). Dredge catches of pilgrim's scallop (*Pecten jacobaeus* L.) in the eastern Adriatic Sea. *Folia Univ. Agric. Stetin.* 192, 37–43.

Chauvaud, L., Lorrain, A., Dunbar, R. B., Paulet, Y.-M., Thouzeau, G., Jean, F., et al. (2005). Shell of the Great Scallop *Pecten maximus* as a high-frequency archive of paleoenvironmental changes. *Geochem. Geophys. Geosyst* 6, Q08001. doi: 10.1029/2004GC000890

Chauvaud, L., Patry, Y., Jolivet, A., Cam, E., Le Goff, C., Strand, Ø., et al. (2012). Variation in size and growth of the Great Scallop *Pecten maximus* along a latitudinal gradient. *PloS One* 7, e37717. doi: 10.1371/journal.pone.0037717

Clements, J. C., and Hunt, H. L. (2017). Effects of $CO_2$-driven sediment acidification on infaunal marine bivalves: A synthesis. *Mar. Pollut. Bull.* 117, 6–16. doi: 10.1016/j.marpolbul.2017.01.053

Cooley, S. R., Rheuban, J. E., Hart, D. R., Luu, V., Glover, D. M., Hare, J. A., et al. (2015). An integrated assessment model for helping the United States sea scallop (*Placopecten magellanicus*) fishery plan ahead for ocean acidification and warming. *PloS One* 10, e0124145. doi: 10.1371/journal.pone.0124145

Dee, D. P., Uppala, S. M., Simmons, A. J., Berrisford, P., Poli, P., Kobayashi, S., et al. (2011). The ERA-interim reanalysis: Configuration and performance of the data assimilation system. *Q. J. R. Meteorol. Soc.* 137, 553–597. doi: 10.1002/qj.828

Denamiel, C., Pranić, P., Ivanković, D., Tojčić, I., and Vilibić, I. (2021). Performance of the Adriatic Sea and coast (AdriSC) climate component – a COAWST V3.3-based coupled atmosphere-ocean modelling suite: Atmospheric part. *Geosci. Model. Dev. Discuss.* 14, 3995–4017. doi: 10.5194/gmd-2021-3

Denamiel, C., Šepić, J., Ivanković, D., and Vilibić, I. (2019). The Adriatic Sea and coast modelling suite: Evaluation of the meteotsunami forecast component. *Ocean. Model.* 135, 71–93. doi: 10.1016/j.ocemod.2019.02.003

Duncan, P. F., Brand, A. R., Strand, Ø., and Foucher, E. (2016). "Chapter 19 - the European scallop fisheries for *Pecten maximus, Aequipecten opercularis, Chlamys islandica* and *Mimachlamys varia*," in *Developments in Aquaculture and Fisheries Science*, vol. 40 . Eds. S. E. Shumway and G. J. Parsons (Amsterdam: Elsevier), 781–858. doi: 10.1016/B978-0-444-62710-0.00019-5

Dutertre, M., Beninger, P., Barillé, L., Papin, M., Rosa, P., Barillé, A., et al. (2009). Temperature and seston quantity and quality effects on field reproduction of farmed oysters, *Crassostrea gigas*, in Bourgneuf Bay, France. *Aquat. Living. Resour.* 22, 319–329. doi: 10.1051/alr/2009042

Ezgeta-Balić, D., Vrgoč, N., Isajlović, I., Medvešek, D., Vujević, A., Despalatović, M., et al. (2021). Comparison of beam trawl catch, by-catch and discard in fishing and non-fishing areas – a case study from the northern Adriatic Sea. *Mediterr. Mar. Sci.* 22, 108–120. doi: 10.12681/mms.24973

Friedman, I., and O'Neil, J. R. (1977). "Compilation of stable isotope fractionation factors of geochemical interest," in *Data of geochemistry*. Ed. M.

Fleischer (Washington D.C: U.S. Geological Society, Professional Paper KK), 1–11. doi: 10.3133/pp440KK

Fröhlich, L., Siebert, V., Walliser, E. O., Thébault, J., Jochum, K. P., Chauvaud, L., et al. (2022). Ba/Ca profiles in shells of *Pecten maximus* – a proxy for specific primary producers rather than bulk phytoplankton. *Chem. Geol.* 593, 120743. doi: 10.1016/j.chemgeo.2022.120743

Fullarton, J. H. (1896). On the development of the common scallop (*Pecten opercularis* L.). *Rep. Fish. Board. Scot.* 6, 290–299.

Gobler, C. J., DePasquale, E. L., Griffith, A. W., and Baumann, H. (2014). Hypoxia and acidification have additive and synergistic negative effects on the growth, survival, and metamorphosis of early life stage bivalves. *PloS One* 9, e83648. doi: 10.1371/journal.pone.0083648

Gosling, E. M. (2015). *Marine bivalve molluscs* (Oxford: Willey Blackwell).

Götze, S., Bock, C., Eymann, C., Lannig, G., Steffen, J. B. M., and Pörtner, H.-O. (2020). Single and combined effects of the "Deadly trio" hypoxia, hypercapnia and warming on the cellular metabolism of the great scallop *Pecten maximus*. *Comp. Biochem. Physiol. B. Biochem. Mol. Biol.* 243–244, 110438. doi: 10.1016/j.cbpb.2020.110438

Heilmayer, O., Brey, T., Storch, D., Mackensen, A., and Arntz, W. E. (2004). Population dynamics and metabolism of *Aequipecten opercularis* (L.) from the western English channel (Roscoff, France). *J. Sea. Res.* 52, 33–44. doi: 10.1016/j.seares.2003.07.005

Hickson, J. A., Johnson, A. L. A., Heaton, T. H. E., and Balson, P. S. (1999). The shell of the Queen Scallop *Aequipecten opercularis* (L.) as a promising tool for palaeoenvironmental reconstruction: evidence and reasons for equilibrium stable-isotope incorporation. *Palaeogeogr. Palaeoclimatol. Palaeoecol.* 154, 325–337. doi: 10.1016/S0031-0182(99)00120-0

Ivanković, D., Denamiel, C., and Jelavić, D. (2019). Web visualization of data from numerical models and real-time stations network in frame of Adriatic Sea and coast (AdriSC) meteotsunami forecast; in *OCEANS 2019 - Marseille*, (Marseille: IEEE) 1–5. doi: 10.1109/OCEANSE.2019.8867225

Johnson, A. L. A., Valentine, A. M., Schöne, B. R., Leng, M. J., Sloane, H. J., and Janeković, I. (2021). Growth-increment characteristics and isotopic ($\delta^{18}O$) temperature record of sub-thermocline *Aequipecten opercularis* (Mollusca: Bivalvia): Evidence from modern Adriatic forms and an application to early pliocene examples from eastern England. *Palaeogeogr. Palaeoclimatol. Palaeoecol.* 561, 110046. doi: 10.1016/j.palaeo.2020.110046

Katsanevakis, S. (2005). Abundance and spatial distribution of the Mediterranean scallop, *Pecten jacobaeus*, in a marine lake. *Fish. Res.* 76, 417–429. doi: 10.1016/j.fishres.2005.07.004

Laing, I. (2002). Effect of salinity on growth and survival of king scallop spat (*Pecten maximus*). *Aquaculture* 205, 171–181. doi: 10.1016/S0044-8486(01)00663-9

Lavaud, R., Flye-Sainte-Marie, J., Jean, F., Emmery, A., Strand, Ø., and Kooijman, S. A. L. M. (2014). Feeding and energetics of the great scallop, *Pecten maximus*, through a DEB model. *J. Sea. Res.* 94, 5–18. doi: 10.1016/j.seares.2013.10.011

Le Pennec, M., Beninger, P. G., Dorange, G., and Paulet, Y. M. (1991). Trophic sources and pathways to the developing gametes of *Pecten maximus* (Bivalvia: Pectinidae). *J. Mar. Biol. Ass. U.K.* 71, 451–463. doi: 10.1017/S0025315400051705

Mackie, L. A., and Ansell, A. D. (1993). Differences in reproductive ecology in natural and transplanted populations of *Pecten maximus*: Evidence for the existence of separate stocks. *J. Exp. Mar. Biol. Ecol.* 169, 57–75. doi: 10.1016/0022-0981(93)90043-N

Magnesen, T., and Christophersen, G. (2008). Reproductive cycle and conditioning of translocated scallops (*Pecten maximus*) from five broodstock populations in Norway. *Aquaculture* 285, 109–116. doi: 10.1016/j.aquaculture.2008.08.024

Marčeta, T., Da Ros, L., Marin, M. G., Codognotto, V. F., and Bressan, M. (2016). Overview of the biology of *Flexopecten glaber* in the North Western Adriatic Sea (Italy): A good candidate for future shellfish farming aims? *Aquaculture* 462, 80–91. doi: 10.1016/j.aquaculture.2016.04.036

Marguš, D., and Teskeredžić, E. (2005). Attachment of larva, survival and growth of juvenile scallops (*Pecten jacobaeus* Linnaeus 1758) in controlled breeding in Šarina Draga Bay —mouth of the Krka river. *Croatian. J. Fisheries.* 63, 1–14.

Markulin, K., Uvanović, H., Mertz-Kraus, R., Schöne, B. R., Kovač, Ž., Arapov, J., et al. (2020). Spatial variations in Ba/Ca$_{shell}$ fingerprints of *Glycymeris pilosa* along the eastern Adriatic Sea. *Estuar. Coast. Shelf. Sci.* 243, 106821. doi: 10.1016/j.ecss.2020.106821

Martínez, G., Mettifogo, L., Lenoir, R., and Olivares, A. (2000). Prostaglandins and reproduction of the scallop *Argopecten purpuratus*: II. relationship with gamete release. *J. Exp. Zool.* 287, 86–91. doi: 10.1002/1097-010X(20000615)287:1<86::AID-JEZ11>3.0.CO;2-W

Mattei, N., and Pellizzato, M. (1996). A population study on three stocks of a commercial Adriatic pectinid (*Pecten jacobaeus*). *Fish. Res.* 26, 49–65. doi: 10.1016/0165-7836(95)00413-0

Morvezen, R., Charrier, G., Boudry, P., Chauvaud, L., Breton, F., Strand, O., et al. (2016). Genetic structure of a commercially exploited bivalve, the great scallop *Pecten maximus*, along the European coasts. *Conserv. Genet.* 17, 57–67. doi: 10.1007/s10592-015-0760-y

Nardi, A., Benedetti, M., Fattorini, D., and Regoli, F. (2018). Oxidative and interactive challenge of cadmium and ocean acidification on the smooth scallop *Flexopecten glaber*. *Aquat. Toxicol.* 196, 53–60. doi: 10.1016/j.aquatox.2018.01.008

Paulet, Y. M., Lucas, A., and Gerard, A. (1988). Reproduction and larval development in two *Pecten maximus* (L.) populations from Brittany. *J. Exp. Mar. Biol. Ecol.* 119, 145–156. doi: 10.1016/0022-0981(88)90229-8

Peharda, M., Soldo, A., Pallaoro, A., Matić, S., and Cetinić, P. (2003). Age and growth of the Mediterranean scallop *Pecten jacobaeus* (Linnaeus 1758) in the northern Adriatic Sea. *J. Shellfish. Res.* 22, 639–642.

Peharda, M., Thébault, J., Markulin, K., Schöne, B. R., Janeković, I., and Chauvaud, L. (2019). Contrasting shell growth strategies in two Mediterranean bivalves revealed by oxygen-isotope ratio geochemistry: The case of *Pecten jacobaeus* and *Glycymeris pilosa*. *Chem. Geo.* 526, 23–35. doi: 10.1016/j.chemgeo.2017.09.029

Pinardi, N., Allen, I., Demirov, E., De Mey, P., Korres, G., Lascaratos, A., et al. (2003). The Mediterranean ocean forecasting system: First phase of implementation, (1998–2001). *Ann. Geophys.* 21, 3–20. doi: 10.5194/angeo-21-3-2003

Poppe, G. T., and Goto, Y. (2000). *European Seashells: Scaphopoda, bivalvia, Cephalopoda (Vol. 2)* (Hackenheim Germany: ConchBooks).

Pranić, P., Denamiel, C., and Vilibić, I. (2021). Performance of the Adriatic Sea and coast (AdriSC) climate component – a COAWST V3.3-based coupled atmosphere-ocean modelling suite: ocean part. *Geosci. Geosci. Model. Dev.* 14, 5927–5955. doi: 10.5194/gmd-14-5927-2021

Ramos, J. E., Tam, J., Aramayo, V., Briceño, F. A., Bandin, R., Buitron, B., et al. (2022). Climate vulnerability assessment of key fishery resources in the Northern Humboldt Current System. *Sci. Rep.* 12, 4800. doi: 10.1038/s41598-022-08818-5

Román, G., Campos, M. J., and Acosta, C. P. (1996). Relationships among environment, spawning and settlement of Queen scallop in the Ría de Arosa (Galicia, NW Spain). *Aquacult. Int.* 4, 225–236. doi: 10.1007/BF00117384

Román, G., Campos, M. J., Acosta, C. P., and Cano, J. (1999). Growth of the queen scallop (*Aequipecten opercularis*) in suspended culture: Influence of density and depth. *Aquaculture* 178, 43–62. doi: 10.1016/S0044-8486(99)00105-2

Saavedra, C., and Peña, J. B. (2004). Phylogenetic relationships of commercial European and Australasian scallops (*Pecten* spp.) based on partial 16S ribosomal RNA gene sequences. *Aquaculture* 235, 153–166. doi: 10.1016/S0044-8486(03)00442-3

Saavedra, C., and Peña, J. B. (2005). Nucleotide diversity and pleistocene population expansion in Atlantic and Mediterranean scallops (*Pecten maximus* and *P. jacobaeus*) as revealed by the mitochondrial 16S ribosomal RNA gene. *J. Exp. Mar. Biol. Ecol.* 323, 138–150. doi: 10.1016/j.jembe.2005.03.006

Sathyendranath, S., Brewin, R. J. W., Jackson, T., Mélin, F., and Platt, T. (2017). Ocean-colour products for climate-change studies: What are their ideal characteristics? *Remote Sens. Environ.* 203, 125–138. doi: 10.1016/j.rse.2017.04.017

Schneider, C. A., Rasband, W. S., and Eliceiri, K. W. (2012). NIH Image to ImageJ: 25 years of image analysis. *Nat. Methods* 9, 671–675. doi: 10.1038/nmeth.2089

Shchepetkin, A. F., and McWilliams, J. C. (2009). Correction and commentary for "Ocean forecasting in terrain-following coordinates: Formulation and skill assessment of the regional ocean modeling system" by Haidvogel et al., *J. Comput. Phys.*, 227, pp. 3595–3624. *J. Comput. Phys.* 228, 8985–9000. doi: 10.1016/j.jcp.2009.09.002

Shcherban, S. A., and Melnik, A. V. (2020). Size and age characteristics and phenotypic peculiarities of somatic growth of the Black Sea mollusk *Flexopecten glaber ponticus* (Bivalvia, Pectinidae). *Biol. Bull. Russ. Acad. Sci.* 47, 920–929. doi: 10.1134/S1062359020080129

Shumway, S., and Parson, G. J. (2016). *Scallops: Biology, ecology, aquaculture and fisheries* (Oxford: Elsevier).

Skamarock, W. C., Klemp, J. B., Dudhia, J., Gill, D. O., Barker, D. M., Wang, W., et al. (2005). *A description of the advanced research WRF version 2. NCAR technical note NCAR/TN-468+STR* (Boulder, CO: University Corporation for Atmospheric Research). doi: 10.5065/D6DZ069T

Stenni, B., Nichetto, P., Bregant, D., Scarazzato, P., and Longinelli, A. (1995). The $\delta^{18}O$ signal of the northward flow of Mediterranean waters in the Adriatic Sea. *Oceanol. Acta* 18, 319–328.

Stokesbury, K., and Bethoney, N. D. (2020). How many scallops are there and why does it matter? *Front. Ecol. Environ.* 18, 513–519. doi: 10.1002/fee.2244

Talmage, S. C., and Gobler, C. J. (2011). Effects of elevated temperature and carbon dioxide on the growth and survival of larvae and juveniles of three species of Northwest Atlantic bivalves. *PloS One* 6, e26941. doi: 10.1371/journal.pone.0026941

Taylor, A. C., and Venn, T. J. (1979). Seasonal variation in weight and biochemical composition of the tissues of the queen scallop, *Chlamys opercularis*, from the Clyde Sea area. *J. Mar. Biol. Assoc. U.K.* 59, 605–621. doi: 10.1017/s0025315400045628

Thébault, J., and Chauvaud, L. (2013). Li/Ca enrichment in great scallop shells (*Pecten maximus*) and their relationship with phytoplankton blooms. *Palaeogeogr. Palaeoclimatol. Palaeoecol.* 373, 108–122. doi: 10.1016/j.palaeo.2011.12.014

Thébault, J., Jolivet, A., Waeles, M., Tabouret, H., Saboret, S., Pécheyran, P., et al. (2021). Scallop shells as geochemical archives of phytoplankton-related ecological processes in a temperate coastal ecosystem. *Limnol. Oceanogr.* 67, 187–202. doi: 10.1002/lno.11985

Thébault, J., Jolivet, A., Waeles, M., Tabouret, H., Saboret, S., Pécheyran, C., et al. (2022) Scallop shells as geochemical archives of phytoplankton-related ecological processes in a temperate coastal ecosystem. *Limnol. Oceanogr.* 67, 187–202. doi: 10.1002/lno.11985

Topić Popović, N., Beer Ljubić, B., Strunjak-Perović, I., Babić, S., Lorencin, V., Jadan, M., et al. (2020) Seasonal antioxidant and biochemical properties of the Northern Adriatic *Pecten jacobaeus*. *PloS One* 15, e0230539. doi: 10.1371/journal.pone.0230539

Tsotsios, D., Tzovenis, I., Katselis, G., Geiger, S., and Theodorou, J. (2016). Spat settlement of the smooth scallop *Flexopecten glaber* (Linnaeus 1758) and sariegated scallop *Chlamys varia* (Linnaeus 1758) in Amvrakikos Gulf, Ionian Sea (Northwestern Greece). *J. Shellfish. Res.* 35, 467–474. doi: 10.2983/035.035.0219

Vendrami, D. L. J., De Noia, M., Telesca, L., Handal, W., Charrier, G., Boudry, P., et al. (2019). RAD sequencing sheds new light on the genetic structure and local adaptation of European scallops and resolves their demographic histories. *Sci. Rep.* 9, 7455. doi: 10.1038/s41598-019-43939-4

Wilding, C. S., Beaumont, A. R., and Latchford, J. W. (1999). Are *Pecten maximus* and *Pecten jacobaeus* different species? *J. Mar. Biol. Assoc. U.K.*, 79, 949–952. doi: 10.1017/S0025315499001149